한국정밀공학회지 제 30 권 9 호 pp. 943-950 September 2013 / 943
J. Korean Soc. Precis. Eng., Vol. 30, No. 9, pp. 943-950 http://dx.doi.org/10.7736/KSPE.2013.30.9.943
ISSN 1225-9071(Print), ISSN 2287-8769(Online)

접촉열전도재를 도포한 접촉열저항 특성연구

Characterization of Thermal Contact Resistance Doped with Thermal Interface Material

Iswor Bajracharya[1], Yoshimi Ito[2], Wataru Nakayama[3], 문병준[4], 이선규[4,✉]
Iswor Bajracharya[1], Yoshimi Ito[2], Wataru Nakayama[3], Byeong-Jun Moon[4], and Sun-Kyu Lee[4,✉]

1 Department of Mechanical and Industrial Engineering of Vienna University of Technology
2 Tokyo Institute of Technology
3 Thermtech International
4 광주과학기술원 기전공학부 (School of Mechatronics, Gwangju Institute of Science & Technology)
✉ Corresponding author: skyee@gist.ac.kr, Tel: +82-62-715-2388

Manuscript received: 2013.8.1 / Accepted: 2013.8.16

This paper describes the thermal contact resistance and its effect on the performance of thermal interface material. An ASTM D 5470 based apparatus is used to measure the thermal interface resistance. Bulk thermal conductivity of different interface material is measured and compared with manufacturers' data. Also, the effect of grease void in the contact surface is investigated using the same apparatus. The flat type thermal interface tester is proposed and compared with conventional one to consider the effect of lateral heat flow. The results show that bulk thermal conductivity alone is not the basis to select the interface material because high bulk thermal conductivity interface material can have high thermal contact resistance, and that the center voiding affects the thermal interface resistance seriously. On the aspect of heat flow direction, thermal impedance of the lateral heat flow shows higher than that of the longitudinal heat flow by sixteen percent.

Key Words: Thermal Interface Material (접촉열전도재), Thermal Contact Resistance (접촉열저항), Thermal Impedance (열임피던스), Bulk Thermal Conductivity (체적열전도율), Apparent Thermal Conductivity (유효열전도율)

NOMENCLATURE

TIM : Thermal interface material
$LVDT$: Linear variable differential transducer
R_{TIM} : Thermal resistance of interface material (K/W)
R_{c1},R_{c2} : Thermal contact resistance (K/W)
R_{int} : Thermal interface resistance (K/W)
$E(R_c)$: Error in thermal contact resistance measurement (K/W)
ΔT_{int} :Temperature difference across thermal interface material (K)
$E(\Delta T_{int})$:Error in temperature difference across thermal interface material (K)
Θ : Thermal Impedance ($m^2 \cdot K/W$)
t_{TIM} : Thermal interface material thickness (m)
$t_{initial}$: Initial reading of LVDT (m)
t_{final} : Final reading of LVDT (m)
k_{bulk}: Bulk thermal conductivity (W/m·K)
A : Heat conduction area (m^2)
Q : Heat input (W)
E(Q) : Heat loss (W)
x : Distance in heat flux bar (m)
T : Temperature at any position corresponding to x (^oC)
T_{hot} : Temperature of hot end in heat flux bar (^oC)
T_{cold} : Temperature of cold end in heat flux bar (^oC)

1. Introduction

Increasing power density and decreasing physical size are the hallmark of modern computer chips which has led to increased problems in the thermal management of electronic devices. Thermal management is essential to maintain such devices within their specifications. Thermal interface material (TIM) performs a critical role in thermal management of devices. They provide the pathway for the transfer of heat from the components to heat sinks. Therefore, an integral part of the thermal management is the selection of the optimal thermal interface material for a specific application.[1,2]

Heat generated within a semiconductor must be removed to the ambient environment to maintain the junction temperature within safe operating limits. This heat removal process involves conduction from the components package surface to the heat sink that can more efficiently transfer heat to the ambient environment .This heat sink has to be carefully joined to the package to minimize the thermal contact resistance of this newly formed joint.[3]

All practical surfaces have microscopic irregularities such as roughness and frequently macroscopic irregularities such as waviness. Therefore heat flow through such a joint is constrained to occur partly through the actual solid contact spots and partly across the gaps between solid spots.[4] The irregularity of real surface is therefore a primary cause of thermal contact resistance.[3]

Thermal contact resistance of confirming contact surfaces is affected by a number of parameters: surface roughness, presence of interstitial gases or thermal interface material, contact micro-hardness and gas pressure. For confirming contacting surface, thermal contact resistance can be analyzed using the semi-empirical model developed by Bahrami et al.[5] Thermal interface material reduces the thermal contact resistance by filling voids and grooves created by the non-smooth surface topography of the mating surfaces, thus improving the surface contact and the conduction of heat across the interface.[1,6,7] The efficiency of thermal interface materials for reducing thermal interface resistance depends on a number of factors among which thermal conductivity of the materials and its ability to wet the mating surfaces appear to be the most significant.[1]

ASTM D 5470 provides the guidelines to conduct steady state test to measure thermal interface resistance. This standard recommends to use contact pressure in the range of 3 MPa and surface roughness less than 0.4 μm and non-zero flatness.[8-11] However, these standards are far above that is found in real heat sink and processor application. In this paper, the standard specimen provided by ASTM D 5470 was investigated without considering the effect of surface roughness and the effect of thermal contact resistance on the performance of thermal interface material also has been presented through experiment. In order to reflect the real conditions, the contact pressure is applied in the lower range,[12] the effect of grease void is also investigated, and the flat type testing method is proposed and compared with the conventional one.[13,14]

2. Thermal Contact Resistance

The ASTM D-5470 test method is the standard steady state test method to measure thermal interface resistance and bulk thermal conductivity of TIM. The sample is placed in between hot and cold meter bar and steady state heat flux is established in the bar. The thermal interface resistance captured between hot and cold meter bar is given by:

$$R_{\text{int}} = \frac{\Delta T}{Q} \tag{1}$$

where ΔT is the temperature drop (K) across the meter bar and Q is the heat input (W). As shown in Fig. 1, the thermal interface resistance is composed of three resistances in series and can be expressed as follows:

$$R_{\text{int}} = R_{TIM} + R_{C1} + R_{C2} \tag{2}$$

where R_{TIM} is thermal resistance of interface material and R_{c1} & R_{c2} are the original thermal contact resistance (K/W). Thermal resistance of TIM, R_{TIM}, can be further written as:

$$R_{TIM} = \frac{t}{k_{bulk} A} \tag{3}$$

where t and k_{bulk} are the thickness (m) and the bulk

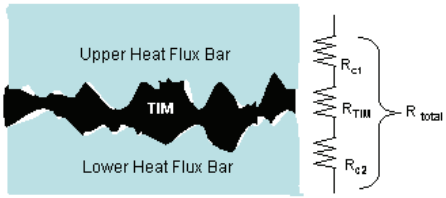

Fig. 1 Thermal interface material between upper and lower heat flux bar

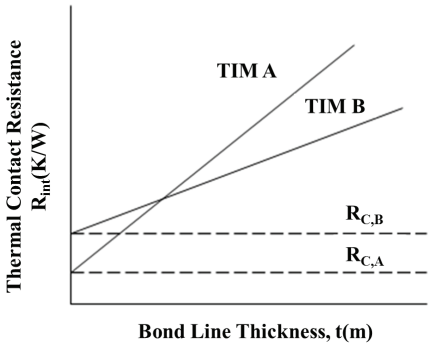

Fig. 2 Example of thermal contact resistance versus thickness for two thermal interface materials

thermal conductivity (W/m-K) of thermal interface material respectively and A is the area of heat transfer (m^2). Substituting the value of R_{TIM} in the Eq.(3) and combining R_{c1} and R_{c2} into R_c, we obtain the following equation:

$$R_{\text{int}} = \frac{t}{k_{bulk} A} + R_c \tag{4}$$

It should be noted that bulk thermal conductivity is independent of thermal interface resistance and material thickness. Eq.(4) represents the equation of straight line where inverse of bulk thermal conductivity, k_{bulk}, is the slope and R_c is the intercept. By collecting the thermal interface resistance over a range of TIM thickness, straight line can be drawn. The inverse of the slope of straight line provides the bulk thermal conductivity of TIM and the intercept provides the thermal contact resistance as shown in Fig. 2.

3. Experiment

Using the guidelines given in ASTM D 5470, a test

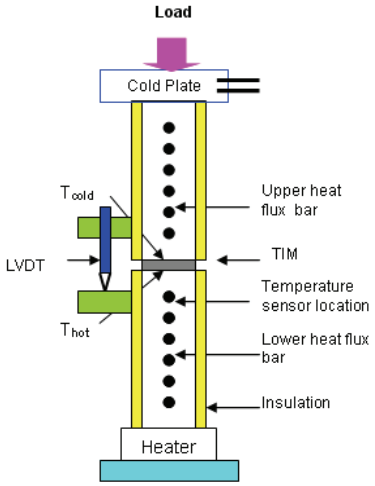

Fig. 3 Schematic of ASTM D 5470 based TIM Tester

apparatus was designed and fabricated. Two cylindrical heat flux bar with heat source and heat sink as shown in Fig. 3 was used. The two heat flux bars are each 100 mm long and 40 mm diameter made of copper. Heat was supplied to the base of the lower heat flux bar from two parallel cartridge heaters, each 150 W. The test surfaces were machined and the measured root mean square roughness was 9.84 μm in lower heat flux bar and 4.36 μm in upper heat flux bar. The flatness was measured to be 0.003º in lower heat flux bar and 0.020º in upper heat flux bar. The heat is conducted vertically upward through the thermal interface material to an upper heat flux bar and then removed by water-cooled heat sink. Five RTD sensors were inserted into 3.5 mm diameter and 20 mm deep holes in the heat flux bar. Thermal interface material is inserted in between two bars and pressure is applied using loading mechanism.

Then plotting the temperature against the position of temperature sensor provides the linear relation with slope equal to dT/dx. The temperature of the joint can be determined by extrapolating the temperature gradient to the joint surface. The temperature of the joint is given by:

$$T = T_0 + \left(\frac{dT}{dx}\right) x \tag{5}$$

where T is temperature at any position corresponding to x, T_0 is temperature at the intercept, dT/dx is slope of straight line (K/m) and x is the distance (m). Through the

extrapolation procedure for lower and upper heat flux bar, the temperature change across the sample, ΔT_{TIM}, can be determined as follows:

$$\Delta T_{TIM} = T_{hot} - T_{cold} \tag{6}$$

Heat input can be measured using power meter or can be calculated using Fourier law of heat conduction. Then thermal interface resistance can be calculated using Eq.(1). Now knowing the thermal interface resistance for range of TIM thickness, graph as shown in Fig. 2 can be plotted. The thickness of TIM can be controlled using thin spacers of different thickness. The bond line thickness of TIM can be measured using LVDT sensor. Initial thickness without TIM is measured at certain value of contact pressure and heat flux. Then final reading with TIM is taken at the same pressure and heat flux level. The difference between the final and initial reading gives the bond line thickness of TIM.

$$t_{TIM} = t_{final} - t_{initial} \tag{7}$$

4. Results and Discussion

4.1 Error analysis

In order to identify the error level of test apparatus, error analysis was done. The relative error in thermal contact resistance is given by (8):

$$\frac{E(R_c)}{R_c} = \left[\left(\frac{E(\Delta T_{\text{int}})}{\Delta T_{\text{int}}} \right)^2 + \left(\frac{E(Q)}{Q} \right)^2 \right]^{1/2} \tag{8}$$

where R_c is thermal contact resistance (K/W), $E(R_c)$ is error in thermal contact resistance measurement (K/W), ΔT_{int} temperature difference across interface material, $E(\Delta T_{int})$ is RTD calibration error plus readout resolution error plus positional uncertainty, Q is heat input (W) and E(Q) is heat loss (W). RTD calibration error as supplied by manufacturer is 0.05 °C; readout resolution error is 0.01 as given in instrument manual; positional uncertainty is 0.01mm from the design of apparatus and heat loss is 2%.

Different thermal interface materials were tested on the apparatus at different heat flux level and relative error was calculated using equation (8). Then the result was plotted in the graph as shown in Fig. 4. This figure shows that:

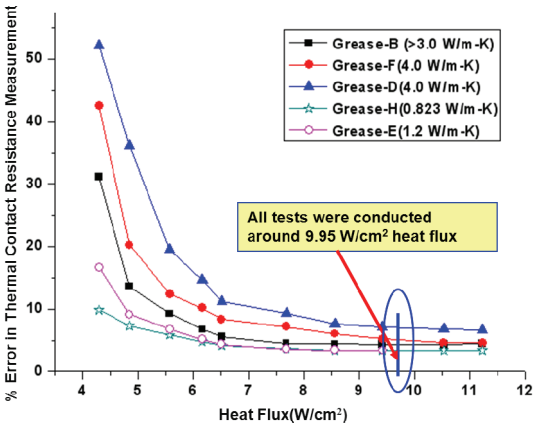

Fig. 4 Error in thermal contact resistance measurement as a function of heat flux for nominal thermal conductivity

1. The measurement error level decreases with increasing heat flux for a specified thermal conductivity material.
2. For a given heat flux, the measurement error is higher for high thermal conductivity material.

In order to minimize the measurement error, all the tests were performed around 10 W/cm^2 heat flux. To accurately acquire the thermal contact resistance data from a variety of interface materials, tests were repeated for five times. Altogether ten samples, of which seven were thermal grease and three were gap pad, were tested to see the effects of thermal contact resistance on their performance.

4.2 Thermal Contact Resistance and Bulk Thermal Conductivity

Thermal interface resistance of TIM was measured over a range of TIM thickness. The thickness of thermal grease was controlled by assembling the test surface with rectangular spacer (1 mm ×1 mm). The spacers were placed at the three places of test surface. The heat transfer through the spacer was assumed negligible as the total heat transfer area of all three spacers together was only 0.23 % of total heat transfer area. The measured thermal

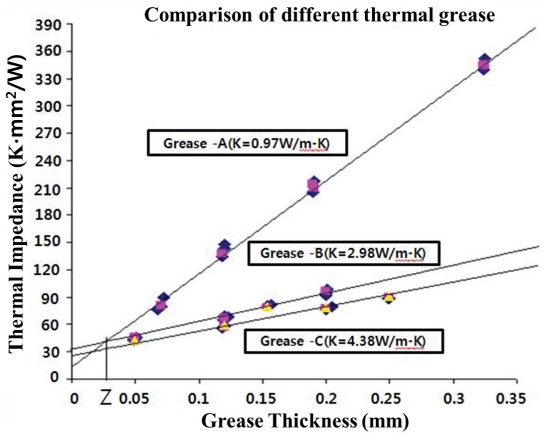

Fig. 5 Effect of grease thickness on the thermal impedance of TIM

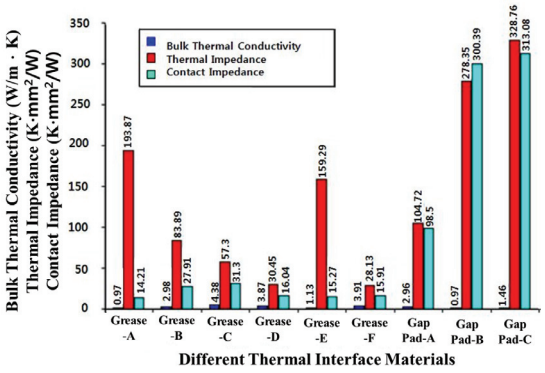

Fig. 6 Comparison of thermal contact impedance of different thermal interface materials

Table 1 Summary of Bulk thermal conductivity and thermal contact resistance of different thermal interface materials

Types of Thermal Interface materials	Bulk thermal Conductivity (measured) (W/m-K)	Bulk thermal Conductivity (catalogue) (W/m-K)	Thermal Contact Resistance (measured) (K/W)
Grease-A	0.97	1.022	0.0113
Grease-B	2.98	>3	0.0222
Grease-C	4.38	>4.5	0.2490
Grease-D	3.87	4	0.0127
Grease-E	1.13	1.2	0.0121
Grease-F	3.91	4	0.0126
Gap Pad-A	2.96	3	0.0783
Gap Pad-B	0.97	1	0.2390
Gap Pad-C	1.46	1.5	0.2491

interface resistance was plotted against the grease thickness and linear relationship was found. Thermal contact resistance and bulk thermal conductivity was evaluated from the best fit line.

Fig. 5 shows the effect of grease thickness on the performance of different thermal grease. Considering the contact area, thermal and contact impedance can be obtained from thermal interface and thermal contact resistance, respectively. Grease A has low bulk thermal conductivity and low contact impedance while grease B has high bulk thermal conductivity and high contact impedance. It can be seen that at grease thickness smaller than z, grease A has smaller thermal impedance as compared to grease B. However, grease B has smaller total thermal impedance than grease A at thickness larger than z. It is considered that this variation is resulted from either the wetness or the microscopic irregularity of mating surfaces. Therefore, it can be said that TIM should be selected not only on the basis of its bulk thermal conductivity but also its contact impedance between the grease and the mating surfaces.

Fig. 6 shows thermal impedance, bulk thermal conductivity and contact impedance of different TIMs. Gap pad- A and grease B have almost same bulk thermal conductivity but contact impedance of gap pad A is very high making its overall performance poorer than that of grease A.

Table 1 shows the summary of bulk thermal conductivity from measured and provided by manufacturer and contact resistance of various thermal interface materials. All tests were conducted at 0.46 MPa and 9.95×10^4 W/m^2 heat flux.

4.3 Apparent Thermal Conductivity

The apparent thermal conductivity was calculated for different TIM thickness and plotted in Fig. 7. Bulk thermal conductivity was also included in the figure for comparison. The figure shows that the value of apparent thermal conductivity is smaller than bulk thermal conductivity but it is gradually increasing with the increase in grease thickness and approaches to the bulk thermal conductivity value. The reason is due to the effect of higher value of contact resistance at smaller

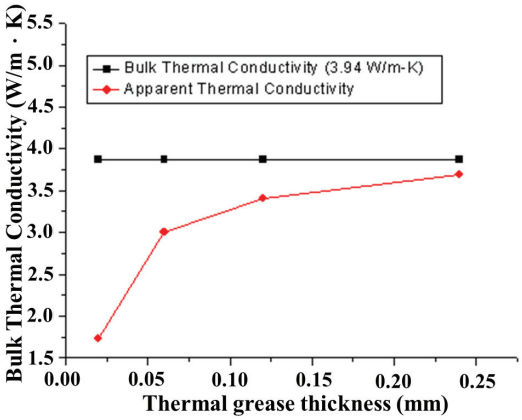

Fig. 7 Comparison between apparent and bulk thermal conductivity for grease D

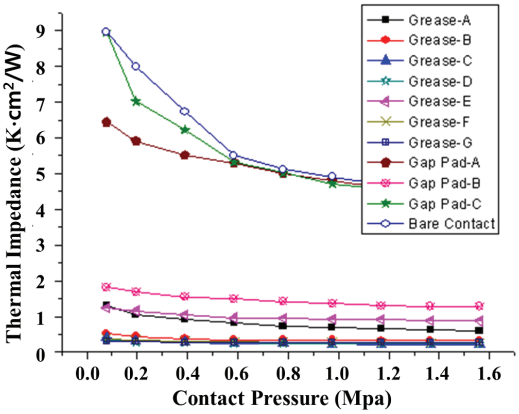

Fig. 8 Effect of contact pressure on thermal impedance

grease thickness. As the grease thickness increases, the effect of contact resistance will be less as compared to the effect of grease thermal resistance.

4.4 Effect of Contact Pressure on Thermal Interface Resistance

Fig. 8 shows the thermal impedance as a function of contact pressure. Thermal impedance decreases in all TIMs as pressure increases, and the thermal impedance of Gap pad is three to four times larger than that of grease. The primary modes are through improved wetting of the contact surface and improved particle to particle contact. It also helps to remove any air that exists within the bond line. Especially gap pad A and gap pad C revealed drastic change of thermal impedance in ordinary packaging

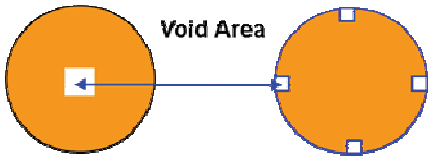

Fig. 9 Center and periphery void area

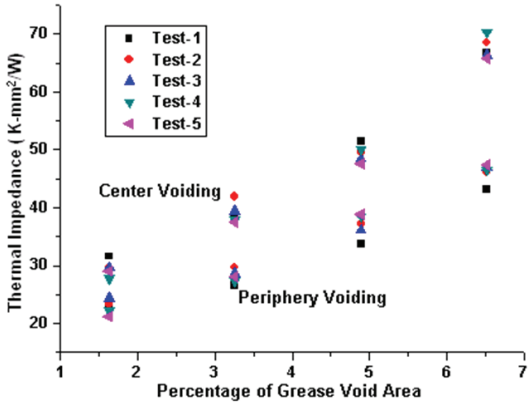

Fig. 10 Effect of void area on the thermal impedance

pressure range. This result indicates that the contact pressure should be applied at least 1.0 MPa to ensure the sufficient heat conduction in case of employing Gap pad.

4.5 Effect of Grease void

In the real system, there may be existed several voids in the contact surface. Experiments were conducted to see the effect of grease voiding at the center and periphery of test surface on the thermal interface resistance.

Rectangular voids were created intentionally while employing grease at the center and periphery of the test surface of apparatus as shown in Fig. 9. A range of void area was defined and calculated using the following relation:

$$Void\ \ area\ \ percentage = \frac{A_2}{A_1} \tag{9}$$

Where A1: Total test surface area(m^2),
A2: Void area(m^2)

The results as shown in Fig. 10 show that for the same void area, thermal contact resistance with center voiding is much higher than with periphery one. It means that center voiding is more serious than periphery voiding.

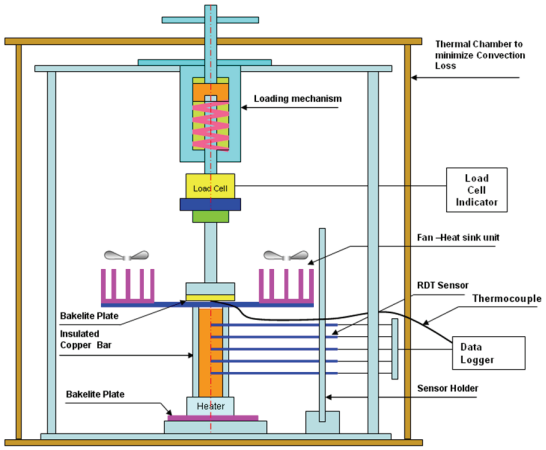

Fig. 11 Experimental set up for flat type thermal interface resistance tester

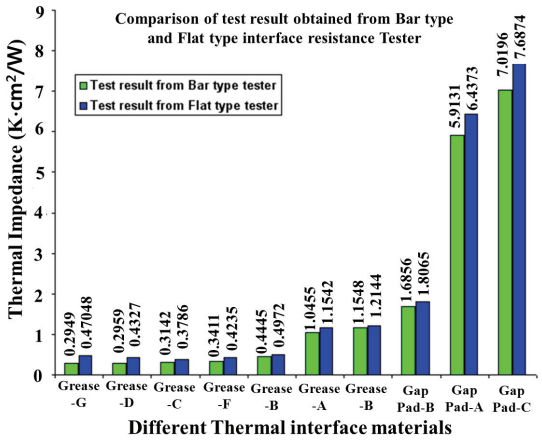

Fig. 12 Comparison of tests results obtained from bar type and flat type TIM tester

4.6 Effect of Heat flow direction

As the ASTM based TIM tester doesn't reflect the realistic user-condition environment, the experiment setup for Flat type TIM tester was designed to ensure realistic characterization of TIM performance in the packaging environment as shown in the Fig. 11.

Water-cooled heat sink and upper heat flux bar were replaced by fan-heat sink unit flat and thin copper plank and long rod with flat plate to apply pressure. The thickness of copper plate is 5.0mm. A flat and thin copper plank with two heat sink placed symmetrically, was used to replicate a heat pipe based thermal solution in notebook system.

Using the temperature shown by sensors and their positions at lower heat flux bar, a linear graph may be plotted and the temperature of hot end can be calculated from extrapolation. Similarly, the temperature of cold side can be obtained from thermocouple reading. Then the thermal interface resistance can be determined dividing this temperature difference by heat input. Experiments were conducted on Flat type TIM tester at 0.39MPa pressure with different types of TIMs.

The results depicted in Fig. 12 show that thermal impedance of the lateral heat flow shows higher than that of the longitudinal heat flow. This can be considered as the effect of a constriction of heat flow. Also, it suggests that ASTM based tester gives an optimistic view of TIM performance that is hard to achieve in real packaging situation.

5. Conclusion

New method of distinguishing the bulk thermal impedance of thermal interface material from the total thermal impedance of interface is suggested and the effect of thermal contact resistance on the performance of thermal interface material was investigated. Based on the ASTM D5470, the smaller thickness is, the higher the effect of thermal contact resistance becomes. As the thickness increases, its effect decreases. The overall performance of thermal interface material may decrease due to the effect of contact resistance even though interface material has high bulk thermal conductivity value. The result shows that bulk thermal conductivity alone is not the basis to select thermal interface material because the contact resistance is different for different thermal interface materials. In addition, center voiding affects the thermal interface resistance significantly. By employing the flat type thermal test apparatus, thermal contact resistance of the lateral heat flow shows higher than that of the longitudinal heat flow by sixteen percent.

ACKNOWLEDGEMENT

This work was financially supported by the National Research Foundation of Korea (NRF) grant funded by the Korea government (MEST) (No.2013006329) and Ministry of Knowledge Economy (MKE) (No.2010-H-003-0030100-2010) and in part supported by Core

Technology Development Program for Next-generation Solar Cells of Research Institute for Solar and Sustainable Energies(RISE), GIST and in part supported by Development of Platform Technology for Machine Accuracy Simulation from the Korea government MKE.

REFERENCES

1. Gwinn, J. P. and Webb, R. L., “Performance and testing of thermal interface materials,” Microelectronics Journal, Vol. 34, No. 3, pp. 215-222, 2003.
2. Grujicic, M., Zhao, C. L., and Dusel, E. C., “The effect of thermal contact resistance on heat management in the electronic packaging,” Applied Surface Science, Vol. 246, pp. 290-302, 2005.
3. Mahajan, R., “Thermal Interface Materials: A Brief Review of Design Characteristics and Materials,” Electronics Cooling, Vol. 2, No. 1, 2004.
4. Madhusudana, C. V., “Accuracy in thermal contact conductance experiments –The effects of heat loss to the surroundings,” International Communications in Heat and Mass Transfer, Vol. 27, No. 6, pp. 877-891, 2000.
5. Bahrami, M., Yovanovich, M. M., and Culham, J. R., “Thermal Joint Resistance of Conforming Rough Surfaces with Gas-filled Gaps,” Journal of Thermophysics and Heat Transfer, Vol. 18, No. 3, pp. 318-325, 2004.
6. Sarvar, F., Whalley, D. C., and Conway, P. P., “Thermal Interface Materials - A Review of the State of the Art,” 1st Electronics Systemintegration Technology Conference, Vol. 2, pp. 1292-1302, 2006.
7. Savija, I., Culham, J. R., and Yovanovich, M. M., “Effective thermophysical properties of thermal interface materials: Part 1 definitions and models,” proc. of International Electronic Packaging Technical Conference and Exhibition, Documet ID: IPACK2003-35088, 2003.
8. Hanson, K., “ASTM D 5470 TIM Material Testing,” IEEE 22nd Annual Semiconductor Thermal Measurement and Management Symposium, pp. 50-53, 2006.
9. Gwinn, J. P., Saini, M., and Webb, R. L., “Apparatus for Accurate Measurement of Interface Resistance of High Performance Thermal Interface Materials,” The 8th Intersociety Conference on Thermal and Thermomechanical Phenomena in Electronic Systems, pp. 644-650, 2002.
10. Kearns, D., “Improving Accuracy and Flexibility of ASTM D 5470 for High Performance Thermal Interface Materials,” 19th IEEE Semiconductor Thermal Measurement and Management Symposium, pp. 129-133, 2003.
11. ASTM D5470-01, “Standard Test Method for Thermal Transmission Properties of Thin Thermally Conductive Solid Electrical Insulation Materials,” 2001.
12. Bahram, M., Yavanovich, M. M., and Culham, J. R., “Thermal contact resistance at low contact pressure: Effect of elastic deformation,” International Journal of Heat and Mass Transfer, Vol. 48, No. 16, pp. 3284-3293, 2005.
13. Kim, J. K., Nakayama, W., and Lee, S. K., “Characterization of a thermal interface material with heat spreader,” J. Korean Soc. Precis. Eng., Vol. 26, No. 1, pp. 91-98, 2010.
14. Kim, J. K., Nam, S.-K., Nakayama, W., and Lee, S. -K., “Compact Thermal Network Model of the Thermal Interface Material Measurement Apparatus With Multi-Dimensional Heat Flow,” IEEE Transactions on Components, Packaging and Manufacturing Technology, Vol. 1, No. 8, pp. 1186-1194, 2011.